Nature of branching in electrohydrodynamic instability

B. Dinesh and R. Narayanan
Department of Chemical Engineering, University of Florida, Gainesville, Florida 32611, USA

(Received 12 November 2020; accepted 20 April 2021; published 10 May 2021)

An electric field imposed on a bilayer of fluids that are stably stratified in the presence of gravity leads to an instability manifested by interfacial deflections. For the case of a perfect conductor underlying a perfect dielectric, an analytical expression obtained from weak nonlinear analysis shows that sinusoidal deflections can only lead to subcritical breakup. While this expression indicates that there is a transition wave number below which supercritical saturation ought to occur, it can be shown that such wave numbers cannot be geometrically accessed, thus precluding any supercritical saturation to steady waves.

DOI: 10.1103/PhysRevFluids.6.054001

I. PHYSICS AND BACKGROUND

Pattern formation due to electrohydrodynamic instability of an interface between conductors and dielectrics is of relevance in the context of lithography [1]. This instability of an interface between a conducting and nonconducting fluid under the influence of a vertical electric field was first analyzed by [2] and electrohydrodynamics has been an active area of research ever since. In this work, we focus our attention on the branching behavior of electrohydrodynamic instability of an interface between two fluids. Whether an interface becomes unstable to steady wave patterns, i.e., to a supercritical branch, or whether it becomes subcritically unstable is of practical significance in the patterning of fluids by electrohydrodynamics. Knowing the conditions and the physical reasons for branching behavior are consequently of importance and the subject of the current study.

As depicted in Fig. 1, the fluids are confined between two rigid plates, where the bottom plate is maintained at a constant voltage D and the top plate is grounded. The applied voltage difference counteracts gravity, which then induces an instability where the conducting fluid assembles into an array of pillars [3–6]. The instability is a consequence of competition between the applied constant potential on the one hand and gravity and surface tension on the other hand. These competing effects can lead to a minimum in a plot of D versus the wave number of the disturbance at the onset of the instability [7]. It has been shown for a conducting-dielectric pair, the case under study, that the viscosities of the fluids play no role at neutral stability ([8]; also see the Supplemental Material [9] for a more general proof). Instead, the destabilizing applied potential is balanced by the stabilizing gravity for low wave numbers, while for high wave numbers, surface tension counteracts the destabilizing potential [7,10]. The competition with surface tension at high wave numbers is reminiscent of the Rayleigh-Taylor (R-T) problem, which is known to lead to a subcritical instability. However, the competition between gravity and electrostatic effects at low wave numbers in the current study is reminiscent of other interfacial instability problems such as the Bénard-Marangoni problem where the instability exhibits supercritical branching [11]. We therefore ask in this work whether there is the possibility of supercritical to subcritical transition at some distinct wave number or whether the instability is always of one of the two types.

There are several studies which are pertinent to the current work. In some of these studies, experiments were performed with polymethylmethacrylate (PMMA) as the conducting fluid and

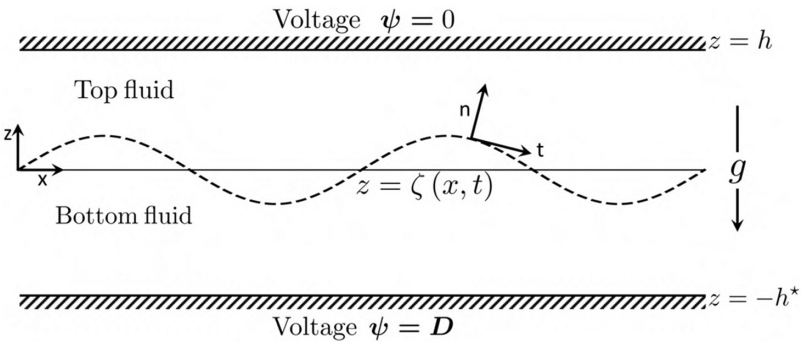

FIG. 1. Schematic of electrostatic instability. The bottom fluid is a perfect conductor and the top fluid is a perfect dielectric. The bottom plate maintains a constant voltage D and the top plate is grounded.

show that PMMA spans the gap between the electrodes upon instability [1,3], thereby indicating subcritical branching. These experimental works were followed by linear stability analyses that also explored the effect of conductivity and thickness of the polymeric fluid [5,12]. Stability of thin polymeric films subject to electrostatic potential was investigated in the long wave limit by [13]. The phenomenon was simulated using both perfect dielectric and leaky dielectric models [14]. A similar study for a bilayer system consisting of two thin leaky dielectric films showed that the viscosity ratio has a significant effect on the evolution of the instability [15]. Nonlinear simulations of these thin bilayer films indicate the formation of pillar-like structures spanning the gap between the electrodes [16], also indicative of subcritical instability. A detailed review of the electrohydrodynamic instability in thin films can be found in [17] and [6].

Observations from the above works show that the pillar formation upon instability spans the gap implying subcritical instability of the interface. The focus of this paper is to prove this mathematically and to provide the physical rationale and conditions for this behavior. To achieve this, we restrict ourselves to the case of a perfect conductor-dielectric pair with the objective of seeking an analytical expression from which we can glean the physics of branching character. To this end, a perturbation series is employed about the neutral state where the applied voltage difference is advanced slightly beyond its critical value.

II. MATHEMATICAL MODEL

The mathematical model refers to a 2-D description of two incompressible, immiscible, Newtonian fluids of infinite lateral extent, lying between two rigid electrically conducting plates located at $-h^\star$ and h, across which a constant voltage difference, D, is applied (cf. Fig. 1). The bottom fluid, represented by an asterisk, is assumed to be a perfect conductor while the top fluid is taken to be a perfect dielectric. The governing equations use length and time scales given by h^* and $t = \frac{h^\star}{U}$ and a potential scale given by D. Here, U is a characteristic velocity scale. It will be seen that the velocity perturbations at the neutral stability state vanish and so the choice of U is ultimately of no consequence in this study. The scaled potential field is given by

$$\nabla^2 \psi = 0. \tag{1}$$

The potential field is subject to a constant value of unity at the bottom plate, i.e., at $z = -1$, while the top plate at $z = \mathcal{H}$ is assumed to be grounded, where $\mathcal{H} = h/h^\star$. The equations of motion are

$$\delta^j \mathrm{Re}\left(\frac{\partial \mathbf{v}^j}{\partial t} + \mathbf{v}^j \cdot \boldsymbol{\nabla}\mathbf{v}^j\right) = -\boldsymbol{\nabla}\mathbf{p}^j + \eta^j \nabla^2 \mathbf{v}^j - \delta^j G \mathbf{i_z}, \tag{2}$$

where the index j represents the bottom fluid (starred) and top fluid (unstarred). Here, $G = \rho^\star g(h^\star)^2/\mu^\star U$, $\mathrm{Re} = \rho^\star U h^\star/\mu^\star$, $\delta^j = \rho^j/\rho^\star$, and $\eta^j = \mu^j/\mu^\star$. No slip and no penetration boundary conditions are imposed on the rigid walls at $z = -1$ and $z = \mathcal{H}$. The common interface is located at $z = \zeta(x,t)$. The velocity components at the interface are equal and the normal and tangential components of the momentum balance hold, i.e.,

$$\mathbf{v}^\star \cdot \mathbf{n} = \mathcal{U} \text{ and } \mathbf{v}^\star = \mathbf{v}, \tag{3}$$

and

$$[[-\mathbf{p}^j\mathbf{I}\cdot\mathbf{n}]] + [[\eta^j\mathbf{T}^H\cdot\mathbf{n}]] - \mathcal{D}(\mathbf{T}^M\cdot\mathbf{n}) = -\frac{1}{\mathrm{Ca}}\mathbf{n}\nabla\cdot\mathbf{n}, \text{ where } \mathrm{Ca} = \mu^\star U/\gamma. \tag{4}$$

Here, the double brackets $[[\phi^j]]$ represent $\phi^\star - \phi$, $\mathbf{I}$ is the identity tensor, and the interfacial speed, $\mathcal{U}$, the unit normal vector, $\mathbf{n}$, and the unit tangent vector, $\mathbf{t}$, are given by

$$\mathcal{U} = \frac{\frac{\partial\zeta}{\partial t}}{\left[1+\left(\frac{\partial\zeta}{\partial x}\right)^2\right]^{1/2}},\ \mathbf{n} = \frac{-\frac{\partial\zeta}{\partial x}i_x + i_z}{\left[1+\left(\frac{\partial\zeta}{\partial x}\right)^2\right]^{1/2}},\ \text{and } \mathbf{t} = \frac{i_x + \frac{\partial\zeta}{\partial x}i_z}{\left[1+\left(\frac{\partial\zeta}{\partial x}\right)^2\right]^{1/2}}. \tag{5}$$

In Eq. (4), the hydrodynamic stress tensor, i.e., $\mathbf{T}^H$, takes its usual form, i.e., $\nabla\mathbf{v}^j + (\nabla\mathbf{v}^j)^t$ and the dimensional form of the Maxwell stress tensor, i.e., $\mathbf{T}^M$ (cf. [14]), is given by $\mathbf{T}^M = \epsilon\epsilon_0\mathbf{EE} - \frac{1}{2}\epsilon\epsilon_0\mathbf{E}\cdot\mathbf{EI}$, where $\mathbf{E} = -\nabla\psi$ is the electric field, ϵ is the relative permittivity of the fluid, and ϵ_0 is the permittivity of free space. The normal component of the Maxwell stress in dimensionless form can be written as

$$(\mathbf{T}^M\cdot\mathbf{n})\cdot\mathbf{n} = \frac{\mathcal{D}}{2}[(\nabla\psi\cdot\mathbf{n})^2 - (\nabla\psi\cdot\mathbf{t})^2], \tag{6}$$

where $\mathcal{D} = \epsilon\epsilon_0 D^2/h^\star\mu^\star U$. For the case of a perfect conductor-dielectric model, there are no tangential components of the Maxwell stress tensor that make a contribution (cf. [14]).

Four key dimensionless groups, i.e., Re, Ca, G, and $\mathcal{D}$, evolve from the nondimensional governing equations and boundary conditions (1)–(6). In what follows, it will become evident that of these groups, GCa and $\mathcal{D}$Ca will combine to form two principal dimensionless groups on account of the base state being quiescent. Our aim is to determine the stability of this simple equilibrium base state and analyze the nature of the bifurcation as we advance a control parameter, viz., $\mathcal{D}$, from its critical value. To this end, we determine the neutral stability conditions and then consider the steady state nature of the branching.

III. NEUTRAL STABILITY

A linear stability analysis of the problem is performed by introducing small perturbations, ψ_1, $\mathbf{v}_1^j$, p_1^j, and ζ_1, about the quiescent base state, via the expansion $\psi(x,z,t) = \psi_0 + \psi_1(z)\cos(kx)e^{\sigma t}$ and similar forms for $\mathbf{v}$, p, and ζ. Here, k is the wave number of the disturbance and the subscript "0" represents the base state fields. To obtain neutral stability, we take σ in the above expansion to be zero on account of exchange of stability. A proof of this is available in the Appendix, where it is also shown that the velocity perturbations are zero at neutral stability or the critical state. This implies that the perturbations need not be other than hydrostatic under critical conditions and is similar to other physical problems that are hydrostatically unstable (e.g., [18–21]). The volume of the fluid is assumed constant, thus requiring that $\int_0^\lambda \zeta\,dx = \text{constant}$, where $\lambda = \frac{2\pi}{k}$ is the disturbance wavelength. Observe that $\mathbf{v}_0^j = \mathbf{0}$ and the base state pressure gradient is thus balanced by the gravitational body force, i.e., $\frac{dp_0^j}{dz} = -\delta^j G$. The base solution for ψ_0 is obtained as $\psi_0 = 1 - z/\mathcal{H}$. As the perturbed velocity is zero we need to only consider the potential field and its effect on the interfacial momentum balance. The linearized equations for the potential field in the

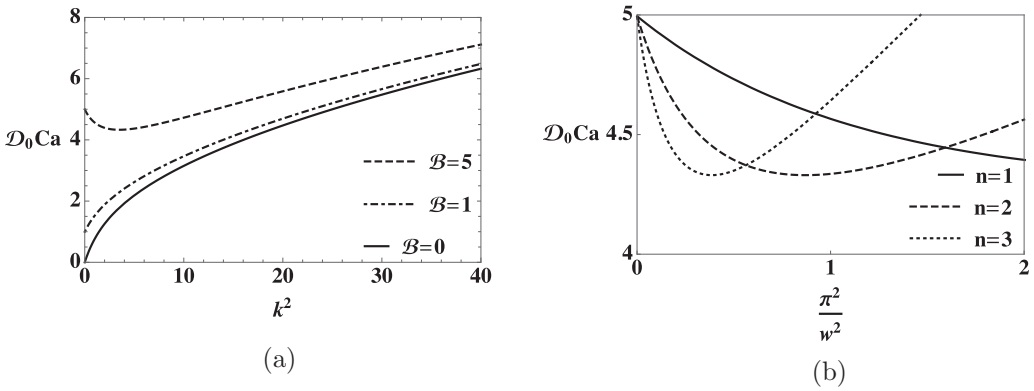

FIG. 2. $\mathcal{D}_0$Ca vs k^2 obtained from Eq. (10). The case of air on top of water is assumed. Panel (a) is drawn for $\mathcal{H} = 1$ and $\mathcal{B} = 0$, 1, and 5. Panel (b) is drawn for $\mathcal{H} = 1$ and $\mathcal{B} = 5$, taking $k = \frac{n\pi}{w}$, with n being the horizontal mode index.

top fluid are given by

$$\left(\frac{d^2}{dz^2} - k^2\right)\psi_1 = 0, \tag{7}$$

where at $z = 0$ and $z = \mathcal{H}$, we have $\psi_1 + \frac{d\psi_0}{dz}\zeta_1 = 0$ and $\psi_1 = 0$. Upon solving Eq. (7), we get

$$\psi_1 = \frac{\zeta_1}{\mathcal{H}}[-\coth(k\mathcal{H})\sinh(kz) + \cosh(kz)]. \tag{8}$$

To determine the neutral stability criteria, we turn toward the perturbed normal component of the momentum balance along the interface, $z = 0$, i.e., Eq. (4),

$$-\frac{dp_0^\star}{dz}\zeta_1 + \frac{dp_0}{dz}\zeta_1 - \mathcal{D}\frac{d\psi_0}{dz}\frac{d\psi_1}{dz} = \frac{-k^2}{\mathrm{Ca}}\zeta_1. \tag{9}$$

Upon substituting the solution for ψ_1, in Eq. (9), we get

$$\underbrace{(1-\delta)G\mathrm{Ca}}_{\equiv\mathcal{B}} + k^2 = \mathcal{D}\mathrm{Ca}\frac{k}{\mathcal{H}^2}\coth(k\mathcal{H}). \tag{10}$$

Here, $(1-\delta)G\mathrm{Ca}$ (also known as the Bond number, $\mathcal{B}$) and $\mathcal{D}\mathrm{Ca}$, hereafter termed $\mathcal{D}_0\mathrm{Ca}$ at the neutral point, can be grouped as pairs and are observed to be independent of the characteristic velocity scale, U, and the viscosities, on account of the perturbed velocity fields being zero under neutral conditions. Typical neutral stability curves obtained from Eq. (10) are shown in Fig. 2(a) drawn for the example of air on top of water (fluid $*$). It can readily be seen from Eq. (10) that the "dip" at high $\mathcal{B}$ is lost when $\mathcal{B} \leqslant 3/\mathcal{H}^2$. Observe, for the case of large $\mathcal{B}$, that on the falling branch of the neutral stability curve, i.e., for low wave numbers, the electrostatic potential driving the instability is balanced by gravity, while on the rising branch, i.e., for high wave numbers, the voltage applied across the horizontal conducting walls is stabilized by interfacial tension. This stabilizing effect of interfacial tension for high wave numbers is analogous to R-T instability of a fluid, wherein the instability is always subcritical in nature. The balance between potential and gravity for low wave numbers is reminiscent of the Bénard instability which is supercritical in nature. Now, not all wave numbers in Fig. 2(a) are accessible. If the curves are monotonic as in the case of small $\mathcal{B}$, the accessible wave numbers are dictated by the horizontal dimensions of the fluid system. However, if the curves display a minimum, the accessible wave numbers, k, depend on the horizontal modal index, n, as displayed in Fig. 2(b) for a one-dimensional system of width, w, where we note that

$k = \frac{n\pi}{w}$. Observe that there are values of w where two consecutive modes may coexist and that to the left and right of these codimension-2 points the curves are nonmonotonic. These special points and the accessible wave numbers in between will play an important part in the conclusions that we shall raise in this study. Our interest, for any of the accessible wave numbers, is to find if and why the instability is super- or subcritical. To determine the nature of the bifurcation, we carry out a weak nonlinear analysis around the bifurcation point, i.e., the critical state.

IV. WEAK NONLINEAR ANALYSIS AND DISCUSSION

To determine the nature of the bifurcation, the dimensionless potential, $\mathcal{D}$, is advanced from its critical value, $\mathcal{D}_0$ by an amount ϵ, such that ϵ is defined by $\mathcal{D} = \mathcal{D}_0 + \frac{\epsilon^2}{2}$. The response of the potential to an increase of the control variable $\mathcal{D}$ is given by $\psi = \psi_0 + \epsilon\psi_1 + \frac{\epsilon^2}{2}\psi_2 + \frac{\epsilon^3}{6}\psi_3 + \cdots$. Likewise for the other state variables such as p^j and ζ. Observe that at $O(\epsilon)$, the first order problem is identical to the perturbed problem at neutral stability given in Sec. III. Therefore at the reference interface, $z = 0$, we get

$$\mathcal{B}\zeta_1 - \frac{\partial^2\zeta_1}{\partial x^2} - \mathrm{Ca}\mathcal{D}_0\frac{d\psi_0}{dz}\frac{d\psi_1}{dz} = 0, \tag{11}$$

where ψ_1 is given by Eq. (8). Hence, $\zeta_1(x)$ is represented by $\zeta_1(x) = \widehat{\zeta_1}\cos(kx)$, where $\widehat{\zeta_1} = \mathcal{A}$ and our objective is to determine the sign of $\mathcal{A}^2$, noting that a positive $\mathcal{A}^2$ indicates a supercritical bifurcation and a negative $\mathcal{A}^2$ implies a subcritical bifurcation (cf. [22]).

The velocity field at the first order is zero as this problem is identical to the perturbed problem which remains in hydrostatic equilibrium. This continues to be true for subsequent higher orders, indicating that the nonlinear problem is an equilibrium problem bearing resemblance to other nonlinear equilibrium problems [18,21]. Noting this, we turn toward the remaining equations at $O(\frac{\epsilon^2}{2})$. The potential field is given by

$$\nabla^2\psi_2 = 0 \tag{12}$$

subject to the following conditions:

$$\psi_2 + \zeta_2\frac{d\psi_0}{dz} = -2\zeta_1\frac{\partial\psi_1}{\partial z}\boxed{+1} \text{ at } z = 0 \text{ and } \psi_2 = 0 \text{ at } z = \mathcal{H}. \tag{13}$$

The normal component of the momentum balance at the interface, $z = 0$, is

$$(p_2 - p_2^\star)\mathrm{Ca} + \mathcal{B}\zeta_2 - \frac{\partial^2\zeta_2}{\partial x^2} - \mathrm{Ca}\mathcal{D}_0\frac{d\psi_0}{dz}\frac{\partial\psi_2}{\partial z} = \mathrm{Ca}\mathcal{D}_0 T_{2f}^{\mathrm{Maxwell}}, \tag{14}$$

where $T_{2f}^{\mathrm{Maxwell}}$ consists of the forcing terms which are bilinear, also called (1,1) terms, because they are products of terms with subscript 1 (cf. the Supplemental Material [9] for the expression of $T_{2f}^{\mathrm{Maxwell}}$). The term $(p_2 - p_2^\star)$, is independent of x because the velocity field is zero. This term is readily calculated by integrating Eq. (14) over a wavelength upon observing that the fluid volume is conserved. The terms associated with $\mathcal{D}_0$ arrive from the expansion of the Maxwell stresses at the second order. We note that all of the forcing terms at this order are bilinear combinations of first order terms, i.e., (1,1) terms with the exception of the boxed term in Eq. (13). This implies that the forcing terms are a superposition of second harmonics, i.e., $\cos(2kx)$ terms and x-independent terms. Their projection onto the eigenspace, i.e., $\cos(kx)$, is zero and thus solvability at second order is automatically satisfied. The boxed term in Eq. (13) is so identified as it is the sole reason for us to determine $\mathcal{A}^2$ at the third order. At the second order, ψ_2 and ζ_2 are expressed as

$$\psi_2 = \widehat{\widehat{\psi_2}}(z)\cos(2kx) + \psi_{20}(z) \text{ and } \zeta_2 = \widehat{\widehat{\zeta_2}}\cos(2kx), \tag{15}$$

where $\widehat{\widehat{\psi_2}}(z)$ is given by

$$\widehat{\widehat{\psi_2}}(z) = \frac{\widehat{\widehat{\zeta_2}} + (\widehat{\zeta_1})^2 k \coth(\mathcal{H}k)}{\mathcal{H}} \cosh(2kz) - \frac{\coth(2\mathcal{H}k)(\widehat{\widehat{\zeta_2}} + (\widehat{\zeta_1})^2 k \coth(\mathcal{H}k))}{\mathcal{H}} \sinh(2kz) \tag{16}$$

$$\text{and } \widehat{\widehat{\zeta_2}} = -\frac{\boldsymbol{\mathcal{D}}_0 \mathrm{Ca}(\widehat{\zeta_1})^2 k^2 [\cosh(2\mathcal{H}k) + 2] \mathrm{csch}^2(\mathcal{H}k)}{4\boldsymbol{\mathcal{D}}_0 \mathrm{Ca} k \coth(2\mathcal{H}k) - 2\mathcal{H}^2(\mathcal{B} + 4k^2)} \tag{17}$$

and where $\psi_{20}(z)$ in Eq. (15) is given by

$$\psi_{20}(z) = \boxed{\left(\underbrace{-\frac{(\widehat{\zeta_1})^2 k \coth(\mathcal{H}k)}{\mathcal{H}^2}}_{\boldsymbol{\psi_{20}^{\mathcal{A}}}} - \underbrace{\frac{1}{\mathcal{H}}}_{\boldsymbol{\psi_{20}^{f}}} \right) z} + \left(1 + \frac{(\widehat{\zeta_1})^2 k \coth(\mathcal{H}k)}{\mathcal{H}} \right). \tag{18}$$

For a matter of convenience that will soon become apparent, we split the boxed term in Eq. (18) into two parts. The first is free of $\widehat{\zeta_1}$ and is called ψ_{20}^{f}, and the other contains $\widehat{\zeta_1}$, called $\psi_{20}^{\mathcal{A}}$.

At the third order the potential field is governed by

$$\nabla^2 \psi_3 = 0 \tag{19}$$

subject to $\psi_3 = 0$ at $z = \mathcal{H}$ and the following condition at $z = 0$

$$\psi_3 + \zeta_3 \frac{d\psi_0}{dz} = -3{\zeta_1}^2 \frac{\partial^2 \psi_1}{\partial z^2} - 3\zeta_1 \frac{\partial \psi_2}{\partial z} - 3\zeta_2 \frac{\partial \psi_1}{\partial z} - 3\zeta_2 \zeta_1 \frac{d^2 \psi_0}{dz^2} - 3{\zeta_1}^3 \frac{d^3 \psi_0}{dz^3}. \tag{20}$$

The normal component of the momentum balance along the interface at $z = 0$ gives

$$(p_3 - p_3^\star)\mathrm{Ca} + \mathcal{B}\zeta_3 - \frac{\partial^2 \zeta_3}{\partial x^2} - \mathrm{Ca}\boldsymbol{\mathcal{D}}_0 \frac{d\psi_0}{dz} \frac{\partial \psi_3}{\partial z} = -9 \frac{\partial^2 \zeta_1}{\partial x^2} \left(\frac{\partial \zeta_1}{\partial x} \right)^2 + \mathrm{Ca}\boldsymbol{\mathcal{D}}_0 T_{3f}^{\mathrm{Maxwell}}, \tag{21}$$

where $T_{3f}^{\mathrm{Maxwell}}$ consists of the (1,2) and (1,1,1) forcing terms (cf. the Supplemental Material [9] for the expression of $T_{3f}^{\mathrm{Maxwell}}$). Therefore, at this order, ψ_3 and ζ_3 are expressed as

$$\psi_3 = \widehat{\widehat{\widehat{\psi_3}}}(z)\cos(3kx) + \widehat{\psi_3}(z)\cos(kx) \text{ and } \zeta_3 = \widehat{\widehat{\widehat{\zeta_3}}}\cos(3kx) + \widehat{\zeta_3}\cos(kx). \tag{22}$$

Here, the $\cos(kx)$ part of the third order problem alone plays a role in the determination of $\mathcal{A}^2$ due to the requirement of the solvability condition at the third order [cf. the Supplemental Material [9] for the solution of $\widehat{\psi_3}(z)$]. Analogous to the second order problem, i.e., Eq. (14), the term $(p_3 - p_3^\star)$ can be determined by integration of Eq. (21) and equals zero on account of the forms of Eq. (22). At the third order, solvability requires that the inhomogeneous terms reside in the null space of the homogeneous problem. This yields an expression for $\mathcal{A}^2$, the details of which may be found in the Supplemental Material [9]. We get

$$\frac{1}{\mathcal{A}^2} = \overbrace{\frac{k\tanh(k\mathcal{H})}{8\sinh^3(k\mathcal{H})}[3\beta\sinh(k\mathcal{H}) + \beta\sinh(3k\mathcal{H}) - 5k\cosh(k\mathcal{H}) + k\cosh(3k\mathcal{H})]}^{\mathrm{I}} \underbrace{-\frac{k\coth(k\mathcal{H})}{\mathcal{H}}}_{\mathrm{II}} \underbrace{-\frac{3k^3\mathcal{H}^2\tanh(k\mathcal{H})}{8\boldsymbol{\mathcal{D}}_0\mathrm{Ca}}}_{\mathrm{III}} \tag{23}$$

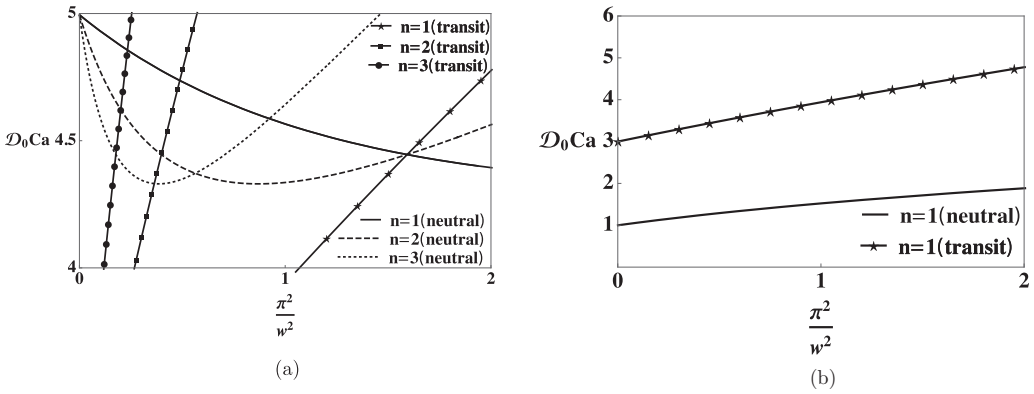

FIG. 3. Graph of $\mathcal{D}_0$Ca vs k^2_{transit} on plots of the neutral stability curves for various horizontal modes n for the case of $\mathcal{B} = 5$ on the left and $\mathcal{B} = 1$ on the right. Allowable wave numbers are to the right of the intersection in (a) and are subcritical. In (b) the k^2_{transit} line lies above the neutral stability curve for low $\mathcal{B}$ implying that all wave numbers are subcritical.

with $\beta = \{k[\cosh(2k\mathcal{H}) + 2]\text{csch}^2(k\mathcal{H})\}/\{[2\tanh(k\mathcal{H})(\mathcal{B} + k^2) - 6k^2\coth(k\mathcal{H})]/(\mathcal{B} + k^2)\}$. Note that $\mathcal{B}$ and $\mathcal{H}$ are inputs to Eq. (23). They are connected to the critical k and Ca$\mathcal{D}_0$ using Eq. (10). These quantities are then used in (23) to determine $\mathcal{A}^2$ and its sign, whence the nature of bifurcation.

A. Key observations from Eq. (23)

Several observations may be made. First, the reason for us to be able to calculate $\mathcal{A}^2$ at the third order is due to the term ψ^f_{20} in Eq. (18). This term arises from the correction of the base state at the second order. Second, the term III in the expression for $\mathcal{A}^2$ corresponds to the trilinear capillary term [first term on the right side of Eq. (21)] in the normal force balance at the third order. This term is always negative indicating the subcritical nature of the bifurcation and plays a key role in the high wave number regime, leading to subcritical branching upon instability. It is analogous to a similar term in the R-T problem. Third, the term II is always negative and arises from $\psi^{\mathcal{A}}_{20}$ in Eq. (18). This term leads to subcritical instability even in the absence of the capillary effects, i.e., term III. Observe that this term is of $O(k)$ unlike term III which is of $O(k^3)$ and so the presence of this term leads to subcritical breakup for smaller k than would otherwise have been seen. Its origin is entirely noncapillary in nature. Fourth, the term I can be traced back to $\hat{\hat{\zeta}}_2$ in Eq. (17) which arises from the normal force balance equation, (14), at the second order. This term contains $\mathcal{B}$ and is a signature of the competition between stabilizing gravity and destabilizing electrostatic potential at low wave numbers. This is the sole term that causes an altering of the sign of $\mathcal{A}^2$, leading to possible supercritical saturation of the interfacial waves. In short, the subcritical nature of the bifurcation is attributed to the capillary terms at the third order and to the second order Maxwell stresses, while this is offset by gravity which counteracts electrostatic potential in the low wave number regime. To see if this offset is powerful enough we set $\mathcal{A}^2$ to zero in Eq. (23) to determine the k^2 where a transition in bifurcation behavior could possibly occur. Denoting these k as k_{transit} and noting that $k = \frac{n\pi}{w}$ we draw the relationship of $\mathcal{D}_0$Ca vs k^2_{transit} and view their intersection against the corresponding neutral stability curves in Figs. 3(a) and 3(b) for the cases of $\mathcal{B} = 5$ and $\mathcal{B} = 1$. All the allowable wave numbers are to the right of the intersections where $\mathcal{B}$ is large and are in regions where the value of $\mathcal{A}^2$ is negative, i.e., subcritical regions. Likewise in the case where $\mathcal{B}$ is small there are no intersections and again all allowable wave numbers must therefore lead to subcritical instability. This means that the term I due to gravity cannot offset the negative nature of the other two terms and we must always see subcritical instability. This result obtains no matter the value of

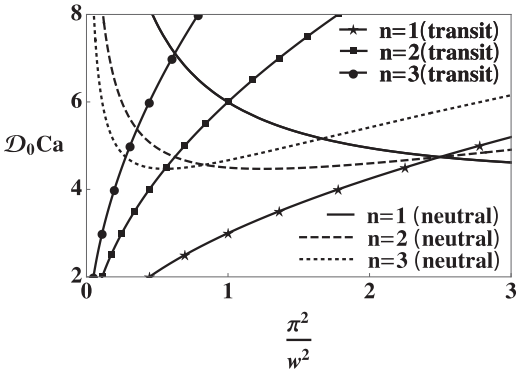

FIG. 4. Figure 3(a) redrawn for the case of deep layers and $\mathcal{B} = 5$.

$\mathcal{B}$ or $\mathcal{H}$. To get a more interpretive formula and an analytical relation for the transit wave number we appeal to a simpler case that retains the essential physics.

B. A simple interpretive formula for the special case of a deep dielectric layer

To further understand the nature of the bifurcation and to glean the physics from a simpler formula, we consider a model where the dielectric fluid is very deep, i.e., much higher than the wavelength of the disturbance. The following expression for $\mathcal{A}^2$ is obtained in the limit of large $k\mathcal{H}$ from Eq. (23) [cf. the Supplemental Material [9] for the derivation of Eq. (24)]:

$$\frac{1}{\mathcal{A}^2} = \underbrace{k\left(\frac{k+\beta}{2}\right)}_{\text{I}} - \underbrace{\frac{k}{\mathcal{H}}}_{\text{II}} - \underbrace{\frac{3k^3\mathcal{H}^2}{8\text{Ca}\mathcal{D}_0}}_{\text{III}}, \quad \text{where } \beta = \frac{k}{\frac{(\mathcal{B}-2k^2)}{(\mathcal{B}+k^2)}}. \tag{24}$$

The companion neutral stability result in this limit is $k\mathcal{D}_0\text{Ca} = (\mathcal{B} + k^2)\mathcal{H}^2$.

Note that the terms I, II, and III in Eq. (24) arise in a manner similar to that of terms I, II, and III in Eq. (23). The wave number corresponding to $\mathcal{A}^2 = 0$ leads to the formula $k_{\text{transit}} = \frac{\mathcal{D}_0\text{Ca}}{3\mathcal{H}^2}$. Figure 4 is the analog of Fig. 3(a) for the case of deep fluid layers, where it is observed that for the case of $n = 1$ the transit line passes through the codimension-2 point between the $n = 1$ and $n = 2$ neutral stability curves. This can also be proven by substitution of the k_{transit} formula into the neutral stability result. We see as before that all accessible wave numbers result only in subcritical instability. This result, whether we use Eq. (23) or Eq. (24), is chiefly due to the fact that the k^2_{transit} curve for $n = 1$ intersects the neutral stability curve to the left of the minimum, i.e., to the left of the "dip." Had it intersected to the right of the minimum, we might have seen supercritical saturation of waves. The nature of the intersection, in this problem, is dominantly affected by term II in the equation for $\mathcal{A}^2$. That is, the intersection to the left of the minimum is due to the electrostatic forcing that is of $O(k)$ overwhelming any possible effect of term I that is $O(k^2)$. Contrast this behavior with the Rayleigh-Taylor instability of a soft gel, where it has been shown by the present authors [23] that the k^2_{transit} line intersects the neutral stability curve to the right of the minimum, depending upon the strength of the elastic forces, affording the possibility of a supercritical instability.

It is noteworthy that the subcritical nature of the bifurcation in the current study is due to the symmetric nature of the sinusoidal disturbances that lead to automatic solvability of Eq. (14) at the second order. However, if hexagonal disturbances were considered (cf. the Christopherson forms given in [24]), it can be shown directly from the solvability condition of Eq. (14) that the nature of the bifurcation must be transcritical. Such a calculation is detailed in the Supplemental Material [9]. Likewise cylindrical waves will lead to subcritical pitchforks when nonaxisymmetric modes result and transcritical branching when axisymmetric modes result (cf. [25] for examples in other

instability problems). It is also noteworthy that the branching behavior observed in the current work stands in contrast with the Rayleigh-Taylor problem of a nonelastic fluid, also an equilibrium problem, where neither hexagonal nor cylindrical disturbances will give rise to transcritical bifurcation as the Rayleigh-Taylor problem for a nonelastic fluid must always bifurcate subcritically.

V. SUMMARY

Using weak nonlinear analysis, it is shown that an electric field imposed on a bilayer of fluids in the presence of gravity can only lead to subcritical instability of the interface. The analysis employs regular perturbation where the perturbation parameter depends on the difference of the applied potential and its critical value. We see that no matter the horizontal dimension of the fluid layers or the Bond number, subcritical branching necessarily results. A simple expression for the case of deep layers reveals that the subcritical nature of the instability is contributed dominantly by electrostatic forcing, which is of $O(k)$, and diminished curvature which is of $O(k^3)$, both being enough to offset the supercritical nature offered by gravity, which is of $O(k^2)$. This study pertains to a conducting-dielectric pair, allowing us to obtain a simple analytical expression that reveals the nature of the bifurcation.

ACKNOWLEDGMENTS

The authors gratefully acknowledge funding from NSF 2025117, NASA via Grants No. NNX17AL27G and No. 80NSSC18K1173, and Florida Space Grant No. 80NSSC20M0093.

APPENDIX: PROOF OF EXCHANGE OF STABILITY

In this Appendix we show that both the real and imaginary parts of the growth rate are zero and that at neutral stability, $\sigma = 0$ also implies that the perturbed velocity and pressure fields are zero. The base interface is taken to be flat but the geometry is taken to be of arbitrary shape. To this end, we consider the vectorial form of the perturbed Navier-Stokes equations for both the fluids, upon assuming perturbations that have a time variation of the form $e^{\sigma t}$ to obtain

$$\sigma \mathrm{Re}\, \mathbf{v_1^\star} = \boldsymbol{\nabla} \cdot \overrightarrow{\overrightarrow{T}}_1^{\,*} + \boldsymbol{\nabla} \cdot \overrightarrow{\overrightarrow{T_1^M}}^{*} \tag{A1}$$

and

$$\sigma \delta\, \mathrm{Re}\, \mathbf{v_1} = \boldsymbol{\nabla} \cdot \overrightarrow{\overrightarrow{T}}_1 + \boldsymbol{\nabla} \cdot \overrightarrow{\overrightarrow{T_1^M}}. \tag{A2}$$

Here,

$$\overrightarrow{\overrightarrow{T}}_1^{\,*} = -p_1^\star \overrightarrow{\overrightarrow{I}} + \overrightarrow{\overrightarrow{S_1^\star}} \quad \text{and} \quad \overrightarrow{\overrightarrow{T}}_1 = -p_1 \overrightarrow{\overrightarrow{I}} + \eta \overrightarrow{\overrightarrow{S_1}}. \tag{A3}$$

For the case of a perfect conductor and a perfect dielectric, $\boldsymbol{\nabla} \cdot \overrightarrow{\overrightarrow{T_1^M}}^{*} = 0$ and $\boldsymbol{\nabla} \cdot \overrightarrow{\overrightarrow{T_1^M}} = 0$. We then take the projection of Eqs. (A1) and (A2) with $\overline{\mathbf{v}^j}$, the complex conjugate of the $\mathbf{v}^j$, and add the resulting equations for each fluid. We obtain

$$\begin{aligned}\sigma \mathrm{Re} \int_{V_0} \mathbf{v_1^\star} \cdot \overline{\mathbf{v}_1^\star}\, dV_0 + \sigma\delta \mathrm{Re} \int_{V_0} \mathbf{v_1} \cdot \overline{\mathbf{v}_1}\, dV_0 &= -\int_{S_0} p_1^\star (\overline{\mathbf{v}_1^\star} \cdot \overrightarrow{n_o})\, dA_0 - \int_{S_0} p_1 (\overline{\mathbf{v}_1} \cdot \overrightarrow{n_o})\, dA_0 \\ + \int_{S_0} \overrightarrow{n_o} \cdot \overrightarrow{\overrightarrow{S}}_1^{\,*} \cdot \overline{\mathbf{v}_1^\star}\, dA_0 + \eta \int_{S_0} \overrightarrow{n_o} \cdot \overrightarrow{\overrightarrow{S}}_1 \cdot \overline{\mathbf{v}_1}\, dA_0 &- \int_{V_0} \overrightarrow{\overrightarrow{S}}_1^{\,*} : \boldsymbol{\nabla} \overline{\mathbf{v}_1^\star}\, dV_0 - \eta \int_{V_0} \overrightarrow{\overrightarrow{S}}_1 : \boldsymbol{\nabla} \overline{\mathbf{v}_1}\, dV_0, \end{aligned} \tag{A4}$$

where V_0 and S_0 represent the volume and interface of the reference domain, i.e., the unperturbed domain and where no slip and no penetration have been used on the rigid surfaces. From Eq. (A4),

we get

$$\sigma \mathrm{Re} \int_{V_0} \mathbf{v_1^\star} \cdot \overline{\mathbf{v}_1^\star}\, dV_0 + \sigma\delta\ \mathrm{Re} \int_{V_0} \mathbf{v_1} \cdot \overline{\mathbf{v}_1}\, dV_0$$
$$= \int_{S_0} \Big(\frac{1}{\mathrm{Ca}} \frac{\partial^2 \zeta_1}{\partial x^2} - (1-\delta) G \zeta_1 + \mathcal{D} \frac{d\psi_0}{dz} \frac{\partial \psi_1}{\partial z} \Big) \overline{\sigma} \overline{\zeta}_1\, dA_0$$
$$- \int_{V_0} \overrightarrow{\overrightarrow{S}}{}_1^* : \nabla \overrightarrow{\overrightarrow{S}}{}_1^*\, dV_0 - \eta \int_{V_0} \overrightarrow{\overrightarrow{S}}{}_1 : \nabla \overrightarrow{\overrightarrow{S}}{}_1\, dV_0. \tag{A5}$$

Likewise we have

$$\overline{\sigma} \mathrm{Re} \int_{V_0} \overline{\mathbf{v}_1^\star} \cdot \mathbf{v_1^\star}\, dV_0 + \sigma\delta \mathrm{Re} \int_{V_0} \overline{\mathbf{v}_1} \cdot \mathbf{v_1}\, dV_0$$
$$= \int_{S_0} \Big(\frac{1}{\mathrm{Ca}} \frac{\partial^2 \overline{\zeta}_1}{\partial x^2} - (1-\delta) G \overline{\zeta}_1 + \mathcal{D} \frac{d\psi_0}{dz} \frac{\partial \psi_1}{\partial z} \Big) \sigma \zeta_1\, dA_0$$
$$- \int_{V_0} \overrightarrow{\overrightarrow{S}}{}_1^* : \nabla \overrightarrow{\overrightarrow{S}}{}_1^*\, dV_0 - \eta \int_{V_0} \overrightarrow{\overrightarrow{S}}{}_1 : \nabla \overrightarrow{\overrightarrow{S}}{}_1\, dV_0. \tag{A6}$$

Adding Eqs. (A5) and (A6), we can write

$$\mathrm{Real}(\sigma) \Bigg[\mathrm{Re} \int_{V_0} |\mathbf{v_1^\star}|^2\, dV_0 + \delta \mathrm{Re} \int_{V_0} |\mathbf{v_1}|^2\, dV_0$$
$$- \int_{S_0} \Big(\frac{1}{\mathrm{Ca}} \frac{\partial^2 \zeta_1}{\partial x^2} - (1-\delta) G \zeta_1 + \mathcal{D} \frac{d\psi_0}{dz} \frac{\partial \psi_1}{\partial z} \Big) \overline{\zeta}_1\, dA_0 \Bigg]$$
$$= - \int_{V_0} \overrightarrow{\overrightarrow{S}}{}_1^* : \nabla \overrightarrow{\overrightarrow{S}}{}_1^*\, dV_0 - \eta \int_{V_0} \overrightarrow{\overrightarrow{S}}{}_1 : \nabla \overrightarrow{\overrightarrow{S}}{}_1\, dV_0. \tag{A7}$$

Hence, $\mathrm{Real}(\sigma) = 0$ implies that $\mathbf{v}_1^j = \mathbf{0}$ as a result of the last two integrals on the right-hand side of Eq. (A7) being single signed. From the kinematic condition along the interface at $z = 0$ [Eq. (3)], we deduce that $\sigma = 0$. This therefore implies that, under neural stability conditions, both the real and imaginary parts of σ are zero and that both perturbed velocity fields are also zero.

[1] E. Schäffer, T. Thurn-Albrecht, T. P. Russell, and U. Steiner, Electrically induced structure formation and pattern transfer, Nature (London) **403**, 874 (2000).

[2] G. I. Taylor and A. D. McEwan, The stability of a horizontal fluid interface in a vertical electric field, J. Fluid Mech. **22**, 1 (1965).

[3] S. Y. Chou and L. Zhuang, Lithographically induced self-assembly of periodic polymer micropillar arrays, J. Vac. Sci. Technol., B: Microelectron. Nanometer Struct.–Process., Meas., Phenom. **17**, 3197 (1999).

[4] S. A. Roberts and S. Kumar, AC electrohydrodynamic instabilities in thin liquid films, J. Fluid Mech. **631**, 255 (2009).

[5] P. Gambhire and R. M. Thaokar, Role of conductivity in the electrohydrodynamic patterning of air-liquid interfaces, Phys. Rev. E **86**, 036301 (2012).

[6] D. T. Papageorgiou, Film flows in the presence of electric fields, Annu. Rev. Fluid Mech. **51**, 155 (2019).

[7] K. Ward, S. Matsumoto, and R. Narayanan, The electrostatically forced Faraday instability: Theory and experiments, J. Fluid Mech. **862**, 696 (2019).

[8] D. H. Michael, Free surface instability in electrohydrodynamics, in *Mathematical Proceedings of the Cambridge Philosophical Society*, Vol. 64 (Cambridge University Press, 1968), pp. 527–534.

[9] See Supplemental Material at http://link.aps.org/supplemental/10.1103/PhysRevFluids.6.054001 for details of the weak nonlinear analysis.
[10] D. Koulova-Nenova, EHD instability of two liquid layer system with deformable interface, J. Electrost. **40**, 185 (1997).
[11] P. Colinet, J. C. Legros, and M. G. Velarde, *Nonlinear Dynamics of Surface-Tension-Driven Instabilities* (Wiley-VCH, Berlin, 2001).
[12] L. F. Pease III and W. B. Russel, Linear stability analysis of thin leaky dielectric films subjected to electric fields, J. Non-Newtonian Fluid Mech. **102**, 233 (2002).
[13] L. F. Pease III and W. B. Russel, Electrostatically induced submicron patterning of thin perfect and leaky dielectric films: A generalized linear stability analysis, J. Chem. Phys. **118**, 3790 (2003).
[14] D. A. Saville, Electrohydrodynamics: The Taylor-Melcher leaky dielectric model, Annu. Rev. Fluid Mech. **29**, 27 (1997).
[15] V. Shankar and A. Sharma, Instability of the interface between thin fluid films subjected to electric fields, J. Colloid Interface Sci. **274**, 294 (2004).
[16] R. V. Craster and O. K. Matar, Electrically induced pattern formation in thin leaky dielectric films, Phys. Fluids **17**, 032104 (2005).
[17] R. V. Craster and O. K. Matar, Dynamics and stability of thin liquid films, Rev. Mod. Phys. **81**, 1131 (2009).
[18] O. A. Basaran and L. E. Scriven, Axisymmetric shapes and stability of isolated charged drops, Phys. Fluids A: Fluid Dynamics **1**, 795 (1989).
[19] X. Lin, L. E. Johns, and R. Narayanan, Static stability of pendent drops pinned to arbitrary closed curves, Phys. Rev. Fluids **2**, 113605 (2017).
[20] S. Chandrasekhar, *Ellipsoidal Figures of Equilibrium* (Yale University Press, 1969).
[21] L. E. Johns and R. Narayanan, *Interfacial Instability* (Springer Science & Business Media, 2007).
[22] P. Grindrod, *The Theory and Applications of Reaction-Diffusion Equations: Patterns and Waves* (Clarendon Press, 1996).
[23] B. Dinesh and R. Narayanan, Branching behavior of the Rayleigh-Taylor instability in linear viscoelastic fluids, J. Fluid Mech. **915**, A63 (2021).
[24] S. Chandrasekhar, *Hydrodynamic and Hydromagnetic Stability* (Clarendon, 1961).
[25] D. D. Joseph, *Stability of Fluid Motions II*, Springer Tracts in Natural Philosophy (Springer, 1976).